fermentation

MDPI

Article

Metabolic Engineering of *Zymomonas mobilis* for Acetoin Production by Carbon Redistribution and Cofactor Balance

Weiwei Bao [1], Wei Shen [2,*], Qiqun Peng [1], Jun Du [3] and Shihui Yang [1,*]

[1] State Key Laboratory of Biocatalysis and Enzyme Engineering, School of Life Sciences, Hubei University, Wuhan 430062, China
[2] School of Life and Technology, Wuhan Polytechnic University, Wuhan 430023, China
[3] China Biotech Fermentation Industry Association, Beijing 100833, China
* Correspondence: wei.shen@whpu.edu.cn (W.S.); shihui.yang@hubu.edu.cn (S.Y.)

Abstract: Biorefinery to produce value-added biochemicals offers a promising alternative to meet our sustainable energy and environmental goals. Acetoin is widely used in the food and cosmetic industries as taste and fragrance enhancer. The generally regarded as safe (GRAS) bacterium *Zymomonas mobilis* produces acetoin as an extracellular product under aerobic conditions. In this study, metabolic engineering strategies were applied including redistributing the carbon flux to acetoin and manipulating the NADH levels. To improve the acetoin level, a heterologous acetoin pathway was first introduced into *Z. mobilis*, which contained genes encoding acetolactate synthase (Als) and acetolactate decarboxylase (AldC) driven by a strong native promoter *Pgap*. Then a gene encoding water-forming NADH oxidase (NoxE) was introduced for NADH cofactor balance. The recombinant *Z. mobilis* strain containing both an artificial acetoin operon and the *noxE* greatly enhanced acetoin production with maximum titer reaching 8.8 g/L and the productivity of 0.34 $g \cdot L^{-1} \cdot h^{-1}$. In addition, the strategies to delete *ndh* gene for redox balance by native I-F CRISPR-Cas system and to redirect carbon from ethanol production to acetoin biosynthesis through a dcas12a-based CRISPRi system targeting *pdc* gene laid a foundation to help construct an acetoin producer in the future. This study thus provides an informative strategy and method to harness the NADH levels for biorefinery and synthetic biology studies in *Z. mobilis*.

Keywords: *Zymomonas mobilis*; acetoin; metabolic engineering; cofactor balance; *noxE*

check for updates

Citation: Bao, W.; Shen, W.; Peng, Q.; Du, J.; Yang, S. Metabolic Engineering of *Zymomonas mobilis* for Acetoin Production by Carbon Redistribution and Cofactor Balance. *Fermentation* **2023**, *9*, 113. https://doi.org/10.3390/fermentation9020113

Academic Editors: M. Ahsanul Islam, Williams Olughu and Donatella Cimini

Received: 19 December 2022
Revised: 19 January 2023
Accepted: 23 January 2023
Published: 25 January 2023

Copyright: © 2023 by the authors. Licensee MDPI, Basel, Switzerland. This article is an open access article distributed under the terms and conditions of the Creative Commons Attribution (CC BY) license (https://creativecommons.org/licenses/by/4.0/).

1. Introduction

Acetoin, also known as 3-hydroxy-2-butanone, is widely used as a food flavoring and fragrance, giving a buttery taste [1]. As a member of the C4-dicarboxylic acid family, acetoin could serve as a high value-added platform for the cosmetics, pharmaceutical, and chemical industries, and the U.S. Department of Energy (DOE) defined acetoin as one of the top 30 platform chemicals [2,3]. As a consequence, many efforts including chemical synthesis, enzymatic conversion, and microbial fermentation have been reported to produce acetoin. Due to safety concerns, the use of non-natural acetoin is restricted in food and cosmetic industries. With the increasing consumption of natural acetoin, there is a thriving demand for sustainable and secure utilization of microorganisms for the production of renewable chemicals [1,3,4].

Many microorganisms, such as *Bacillus subtilis* [5], *Bacillus amyloliquefaciens* [6], *Enterobacter cloacae* [7], *Serratia marcescens* [8], *Zymomonas mobilis* [9], *Saccharomyces cerevisiae* [10] and *Paenibacillus polymyxa* [11] have been found to excrete acetoin as a physiological metabolite. For instance, Acetoin and diacetyl are aroma compounds that are produced during alcoholic fermentation in yeast, which contributes to the organoleptic and textural profile of the fermented foods [3]. In *S. cerevisiae*, pyruvate is more likely converted into ethanol other than acetoin under anaerobic conditions. The acetoin production was improved by

experimental design and performed under aerobic conditions [3]. Acetoin plays a crucial role in the regulation of the NADH/NAD^+ ratio, and is used as an external energy storage by many fermentative bacteria [1,12]. Acetoin not only serves critical roles in yeast osmoregulation and redox balancing, but also acts as the carbon competitor against ethanol in alcoholic fermentation. A certain amount of acetoin accumulates during the period of main fermentation, which is then reduced by the yeast. The consumption of acetoin during fermentation may result from the redox balancing. The introduction of heterologous acetoin biosynthesis pathway into *S. cerevisiae* and deletion of byproduct pathways benefited for acetoin yield and productivity [10].

Three pathways have been reported for acetoin production (Figure 1). (i) Acetoin can be generated from the intermediate alpha-acetolactate of the branched-chain amino acids pathway. Two molecules of pyruvate are condensed to form one α-acetolactate by acetolactate synthase (Als). Acetolactate is an unstable compound, the biologically active substance is further converted to acetoin by acetolactate decarboxylase (AldC). (ii) Acetolactate is converted to diacetyl by nonenzymatic oxidative chemical decarboxylation (NOD), and diacetyl can be further reduced to acetoin by acetoin dehydrogenase (ButA) using NADH/NAD^+ ascoenzyme [1,13]. (iii) Pyruvate decarboxylase (PDC) takes part in carboligase activity reaction (CAR). PDC catalyzes the irreversible non-oxidative decarboxylation of pyruvate to produce acetaldehyde and can also catalyze an aldol-type condensation reaction between "active acetaldehyde" and free acetaldehyde to form acetoin [14,15]. Acetoin dehydrogenase (ButA) belong to the SDR (short-chain dehydrogenases/reductases family), which are enzymes of ≈250 residue subunits and known to be NAD(P)(H)-dependent oxidoreductases [16,17].

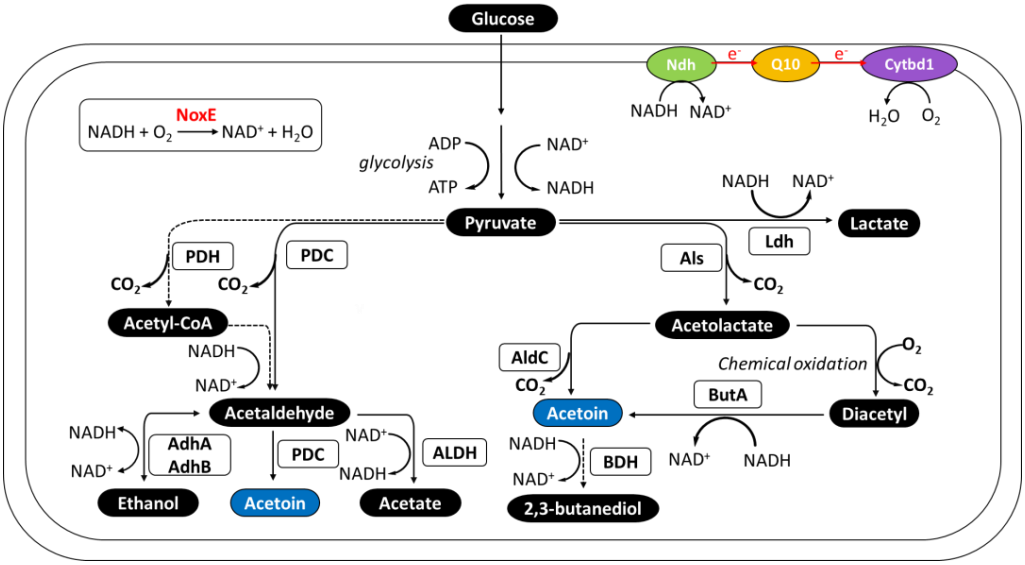


Figure 1. The native glycolysis and ethanol production pathways in *Z. mobilis* and potential acetoin biosynthesis pathways. The native pathways of *Z. mobilis* are shown with solid line, and heterologous pathways are shown with dashed lines. NoxE (Red color font) is a heterologous NADH oxidase. AdhA/B, alcohol dehydrogenase; AldC, acetolactate decarboxylase; ALDH, Aldehyde dehydrogenase; Als, acetolactate synthase; BDH, 2,3-butanediol dehydrogenase; ButA, Acetoin dehydrogenase; Ldh, lactate dehydrogenase; PDC, pyruvate decarboxylase; PDH, pyruvate dehydrogenase.

Z. mobilis is a natural ethanologenic bacterium, which is generally regarded as safe (GRAS) and well known for its high specific glucose uptake rate and rapid sugar catabolism [18]. Notably, *Z. mobilis* has truncated tricarboxylic acid cycle (TCA cycle), more than 95% of the carbon flux is oriented to ethanol production by PDC in *Z. mobilis*, and branch metabolic pathways compete for substrate binding and utilization. When performing aerobic fermentation, *Z. mobilis* converts pyruvate to ethanol, lactic acid, acetic acid, and

acetoin as the end products [19,20]. As oxygen content increased, acetoin yields also increased. However, the spontaneous chemical reaction is uncontrollable and leads to deficient aerobic growth.

Acetoin can be further converted to 2,3-butanediol (2,3-BDO) by 2,3-butanediol dehydrogenase (BDH) using NADH as cofactor (Figure 1). A heterologous 2,3-butanediol biosynthesis pathway was introduced into *Z. mobilis* with a titer of 13 g/L achieved [21]. However, the yield of 2,3-BDO and ethanol were reduced with the increasing oxygen levels. It was speculated that the amino acids branched 2,3-BDO biosynthesis pathway reduced the generation of NAD^+, and increased the NADH/NAD^+ ratio, which could then reduce the glycolysis efficiency and cellular growth. It was reported that acetoin and 2,3-butanediol were converted into each other using NADH/NAD^+ as coenzyme [22].

Nevertheless, acetoin is an oxidized product. which plays a crucial role in the regulation of the NADH/NAD^+ ratio and is used as an external energy store by several fermentative bacteria. In the acetoin pathway, NADH produced from glycolysis could not be converted to NAD^+ leading to a redox cofactor imbalance [12,23]. The unbalanced NADH/NAD^+ ratio hinders the conversion of acetaldehyde to ethanol, and the accumulation of acetaldehyde will be toxic to cells. Thus, maintaining cofactor balance is crucial to sustaining cellular metabolism and helps improve acetoin production.

It is reported that NADH oxidase (NoxE) catalyzes the oxidation of NADH to NAD^+ using molecular oxygen as the electron acceptor, and it is favored to be introduced to the NADH-dependent pathways [24,25] for NADH and NAD^+ balance. For example, gene encoding NoxE was integrated into the acetoin biosynthetic pathway of *S. cerevisiae* to catalyze the oxidation of NADH to NAD^+. The yield of acetoin in *S. cerevisiae* has been greatly improved via the cofactor engineering strategy [10].

In this work, an integrated strategy of introducing genes for heterologous acetoin biosynthesis and redox balance was used to improve acetoin production, which included the introduction of acetolactate synthase (Als) and acetolactate decarboxylase (AldC) to redistribute the metabolic flux for acetoin production and the introduction of an NADH oxidase (NoxE) for NADH/NAD^+ balance to provide NAD^+ for efficient glycolysis and cell growth in *Z. mobilis* while reducing other NADH-dependent products such as ethanol and other byproducts of lactic acid and acetate.

2. Materials and Methods

2.1. Strains Plasmids and Cultural Conditions

All bacterial strains and plasmids used in this study are listed in Table 1. *Z. mobilis* ZM4 and its derivatives were cultivated in rich media supplemented with 5% glucose (RMG5, 50 g/L glucose, 10 g/L yeast extract, 2 g/L KH_2PO_4) at 30 °C. *Escherichia coli* XL10-Gold was cultured in Lysogeny broth (LB, 10 g/L NaCl, 10 g/L tryptone, 5 g/L yeast extract) and used for plasmid construction. *E. coli* ET12567 was used as a non-methylation plasmid donor for delivering plasmids to *Z. mobilis* strains. Shuttle vector pEZ15Asp containing origins of replication for both *E. coli* and *Z. mobilis* was used for pathway engineering.

2.2. DNA Manipulation Techniques

Gibson assembly method was utilized for all plasmid construction. All constructs used in the study are listed in Table 1. Primers were designed to contain 15–20 nucleotides (nts) overlapping regions with adjacent DNA fragments. The oligonucleotides of primers were ordered from TsingKe Biotechnology Co., Ltd. (Beijing, China). Sequences of the primers are listed in Table 1. Plasmid DNA was extracted using AxyPrep kits (Corning, Shanghai, China). DNA polymerases used were PrimerSTAR (Takara, Kyoto, Japan) or Taq DNA polymerases (Tsingke, Beijing, China). Recombinants were confirmed by PCR and Sanger sequencing (Tsingke, Beijing, China).

Table 1. Strains, plasmids and primers used in this study.

Strains, Plasmids and Primers	Description	Source
Strain		
E. coli XL10-Gold	*TetrΔ(mcrA)183Δ, Δ(mcrCBhsdSMR-mrr)173, endA1, supE44,thi-1,recA1,gryA96relA1,lacHte [F', proAB, lacIq ZΔM15, Tn10::Tet', Camr]*	Invitrogen
E. coli ET12567	*F- dam-13::Tn9 dcm-6 hsdM hsdR zjj-202::Tn10 recF143 galK2 galT22 ara-14 lacY1 xyl-5 leuB6 thi-1 tonA31 rpsL136 hisG4 tsx-78 mtl-1 glnV44*	Lab stock
ZM4	*Z. mobilis* subsp. *mobilis* ZM4, wild-type	Lab stock
ZM4Δ1113	*Z. mobilis* ZM4, *ZMO1113* deletion mutant	This study
ZM4 (pEZ)	ZM4 containing pEZ	This study
ZM4 (pEZ-NoxE)	ZM4 containing pEZ-NoxE	This study
ZM4 (pEZ-AldC)	ZM4 containing pEZ-AldC	This study
ZM4 (pEZ-AldC-Als)	ZM4 containing pEZ-AldC-Als	This study
ZM4 (pEZ-AldC-Als-NoxE)	ZM4 containing pEZ-AldC-Als-NoxE	This study
ZM4-1759dCas12a (pEZ-AldC-Als-NoxE)	ZM4 (pEZ-AldC-Als-NoxE) with ZMO1759 replaced by gene *dCas12a*	This study
ZM4Δ1113 (pEZ-AldC-Als-NoxE)	ZM4Δ1113 containing pEZ-AldC-Als-NoxE	This study
Plasmid		
pEZ	pEZ15Asp, *P15A_ori*, *Zymo_Ori*, spe^r	[21]
pEZ-NoxE	*P15A_ori*, *Zymo_Ori*, P_{pdc}*::noxE*, spe^r	This study
pEZ-AldC	*P15A_ori*, *Zymo_Ori*, P_{gap}*:: EcaldC*, spe^r	This study
pEZ-AldC-Als	*P15A_ori*, *Zymo_Ori*, P_{gap}*:: EcaldC*, P_{tet}*::Bsals*, spe^r	This study
pEZ-AldC-Als-NoxE	*P15A_ori*, *Zymo_Ori*, P_{gap}*:: EcaldC*, P_{tet}*::Bsals*, P_{pdc}*::noxE*, spe^r	This study
pEZ-sgr	*P15A_ori*, *Zymo_Ori*, spe^r, containing miniCRISPR of CRISPR–Cas12a system	[26]
pST	*P15A_ori*, *Zymo_Ori*, spe^r, containing miniCRISPR of endogenous Type I-F CRISPR–Cas system	[27]
Primer	Oligo Sequence (5′ → 3′)	
NoxE-F	tttttctttgtgagtccaatgaaaatcgtagttatcggtacg	This study
NoxE-R	cagcggccgctactagtattattttgcatttaaagctgcaacag	This study
AldC-F	aattcgcggccgcttctattactcgggattgccttcg	This study
AldC-R	cagcggccgctactagtactatgagtgttgatctgagatttcg	This study
Als-F	tactagtagcggccgctg	This study
Als-R	cagcggccgctactagtattacagagctttcgttttcatcagttc	This study
1113US-F	accagctcaccgtctttggcaaatccgaaaacggc	This study
1113US-R	tgcgtcaaatattgaaacctctattctcttccaagcga	This study
1113DS-F	aggtttcaatatttgacgcagaagacttttgtagcac	This study
1113DS-R	agatctgatatcactctgataggctctctgccgac	This study
1113check-F	cgggctatgctggctaatca	This study
1113check-R	ggctaagatagcgccgagtt	This study
1113in-R	acgcccaaacgctgtaaaac	This study
dCas12a-F	ctaaatttttttcttcttaagacccactttcacatttaagttgtttttctaatc	This study
dCas12a-R	atgacctattggtggtaaaacgaaaggcccagtctttcgac	This study
1759check-F	gccaacatcatccgaaggga	This study
1759check-R	tatgaatgttattcgctaccggttg	This study

2.3. Cultivation Conditions in Shake Flasks

Seed culture of *Z. mobilis* ZM4 and its derivates were firstly revived from frozen glycerol stocks in RMG5 at 30 °C for 6–8 h without shaking and then inoculated into 100-mL shake flasks containing different volumes of RMG5 at an initial $OD_{600} \approx 0.05$. Except for the wild-type strain ZM4, the medium was supplemented with spectinomycin at a final concentration of 100 μg/mL, and the temperature was maintained at 30 °C. Three or more technical replicates were used for each condition. Samples were taken at various time points for further analysis.

2.4. Construciton of gRNA Constructs for CRISPRi

The construction of dCas12a based CRISPRi gRNA was carried out following published procedures [26]. Briefly, plasmid pEZ-sgr derivative from pEZ15A was used to transcribe target-specific sgRNA in *Z. mobilis*. pEZ-sgr carries a minimal CRISPR array containing two *Bsa*I restriction sites for easy cloning of new spacers. The targeting gRNA sequence was annealed using two single-stranded oligonucleotides and ligated into *Bsa*I-linearized pEZ-sgr.

2.5. Deletion of NAD(P)H Dehydrogenase Genen (ndh) Using Native I-F CRIPSR System

Targeting plasmid pST and derivatives constructed in this work following previous study [27]. Oligonucleotides were designed targeting to *ndh* sequence. The targeting gRNA sequence was annealed using two single−stranded oligonucleotides by first heating the reaction mixture to 95 °C for 5 min and subsequently cooling down gradually to room temperature. Then, the annealed spacer was ligated into pST that was digested with *Bsa* I. Gibson assembly method was utilized for donor construction. Donor sequences including extra ~800 bp upstream and downstream flank sequences of the candidate gene were amplified using Primer STAR polymerase (Takara, Kyoto, Japan) from the genomic DNA of *Z. mobilis* ZM4 and then cloned into corresponding pST targeting *ndh*.

2.6. Identification of ndh Deletion in Z. mobilis

To confirm the deletion of *ndh* in *Z. mobilis*, mutant candidates were identified by colony PCR. A pair of primers was designed to amplify the region including upstream of the corresponding gene, targeting gene, and downstream of the corresponding gene. mutant candidates with correct PCR product sizes were selected as candidates and confirmed by Sanger sequencing (Tsingke, Beijing, China).

2.7. Curing of Targeting Plasmids

In order to cure the targeting plasmid, the mutant harboring the targeting plasmid after genome editing was inoculated into RMG5 medium without antibiotics selection pressure for 8 to 16 h, which were then spread on RMG5 plates without antibiotic. Colonies were confirmed as targeting plasmid cured by determining their sensitivity to chloramphenicol.

2.8. Electroporation for Z. mobilis

The preparation of electrocompetent cells and electroporation for *Z. mobilis* was carried out following published procedures [26]. Briefly, a single colony was inoculated into 5 mL RMG5 media and grown without shaking at 30 °C for 24 h as the seed culture. The seed culture was then transferred to a screw-cap bottle. Cells culture was placed on ice for 30 min and cells were collected by centrifuging when OD_{600} reached 0.4–0.6. Cell pellets were washed once with ice-cold sterile water, re-centrifuged, and washed twice in pre-chilled-sterilized 10% (*v*/*v*) glycerol. These pellets were resuspended in 10% glycerol at a concentration approximately 1000-fold higher than the starting culture. Competent cells were stored at −80 °C as small aliquots for later use. *Z. mobilis* cells were transformed with plasmids by electroporation (Bio-Rad Gene Pulser, 0.1-cm gap cuvettes, 1.6 kV, 200 Ω, 25 μF). After electroporation, 1 mL RMG5 was added to the electroporation mixture and cells were allowed to be recovered at 30 °C for 3–5 h. The revived culture was plated on solid mating media containing appropriate antibiotics and then incubated at 30 °C for 2–3 days. Colonies with correct PCR product sizes were selected as candidates and identified using Sanger sequencing (Tsingke, Beijing, China).

2.9. Analytical Methods

Cell growth was determined by measuring OD_{600} using a UV spectrophotometer (UV-1800, Aoyi, Shanghai, China). To analyze the profile of metabolites, 1 mL culture supernatants were collected and filtered through a 0.22 μm syringe filter. The concentrations of glucose, glycerol, acetoin, acetate, and ethanol were determined by high-performance

liquid chromatography (HPLC) using the Shimadzu HPLC system (Kyoto, Japan) equipped with a Bio-Rad Aminex HPX-87H column (300 mm × 7.8 mm, 5µm, Bio-Rad, CA, USA) at 60 °C and refractive index (RI) detector for compound separation and detection, respectively. H_2SO_4 (5 mM) at a flow rate of 0.5 mL/min was used as the mobile phase, following previous protocol [18].

The intracellular concentrations of NADH and NAD^+ were measured using NAD/NADH Assay Kit (S0175, Beyotime, Shanghai, China). Briefly, strains were harvested and washed with cold phosphate-buffered saline (PBS; 8 g/L NaCl, 0.2 g/L KCl, 1.42 g/L Na_2HPO_4, 0.24 g/L KH_2PO_4, pH 7.4) solution. Samples were homogenized using a Dounce homogenizer (30 ~ 50 passages) with NADH/NAD Extraction Buffer, and supernatants were then collected by centrifuging at 4 °C for 10 min. For measuring total NADH and NAD^+, 20 µL of extracted aliquots and 90 µL of reaction mix were added in each well of a 96-well microplate, incubated at 37 °C for 10 min. 10 µL of NADH developer were added in each well and mixed, incubated at 37 °C for 30 min and OD450nm values were then measured using a microplate reader (Spectro MAX190, Molecular Devices, CA, USA). To detect NADH, extracted aliquots were heated to 60 °C for 30 min in a heating block to decompose NAD^+ before blending with the reaction mix.

3. Results

3.1. Investigation of Fermentation Conditions for Acetoin Production in Z. mobilis

Different flask fermentation conditions were first investigated using the wild-type ZM4. Strains were cultured in shake flakes (30 °C, 100 rpm) with different medium volumes to control the dissolved oxygen content. The 100-mL shake flasks containing 80 mL RMG5 served as an anaerobic condition and 20 mL RMG5 was regarded as aerobic condition. When strains reached the stationary phase, glucose was depleted and end products such as ethanol, acetoin, and acetate reached the maximum levels in both aerobic and anaerobic conditions. Our results indicated that *Z. mobilis* ZM4 reached a maximal cell density under anaerobic fermentation, while the presence of oxygen negatively affected glucose consumption rate and growth (Figure 2, Table 2), which were consistent with the previous report [28].

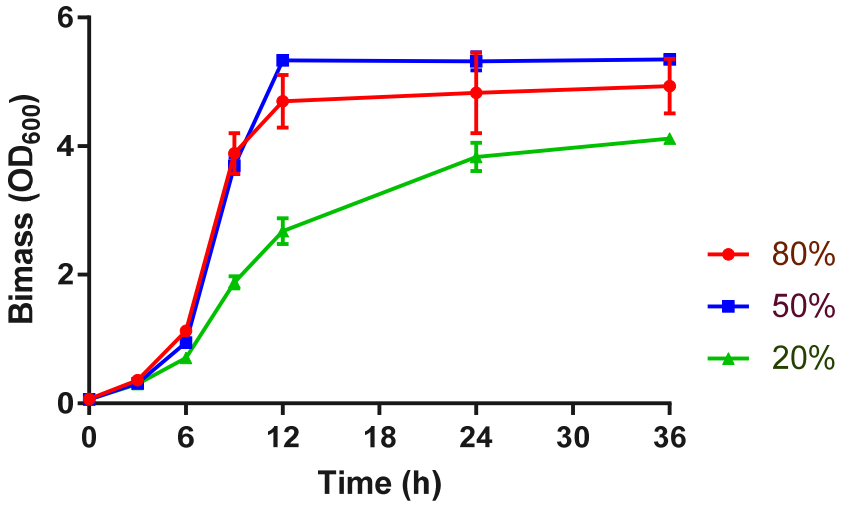


Figure 2. Growth curve of *Z. mobilis* under different conditions. 20%, 50%, and 80% represented corresponding conditions that 100-mL shake flasks contained 20, 50, or 80 mL RMG5, respectively. Values are the means of experiments with three or more technical replicates; error bars are standard deviations.

Table 2. Fermentation profiles of *Z. mobilis* under different conditions. GCR: Glucose consumption rate, GC: Glucose consumed. Strains were cultured in 100-mL shake flakes at 30 °C, 100 rpm. Mean values for triplicate repeats are shown for each condition ± standard deviation.

Volume	GCR ($g \cdot L^{-1} \cdot h^{-1}$)	GC ($g \cdot L^{-1}$)	Ethanol ($g \cdot L^{-1}$)	Acetate ($g \cdot L^{-1}$)	Glycerol ($g \cdot L^{-1}$)	Acetoin ($g \cdot L^{-1}$)	Lactate ($g \cdot L^{-1}$)
80%	4.16 ± 0.24	46.50 ± 0.65	20.61 ± 0.57	0.51 ± 0.18	0.10 ± 0.03	1.21 ± 0.35	1.00 ± 0.06
50%	4.15 ± 0.17	46.57 ± 0.26	20.31 ± 0.29	0.37 ± 0.04	0.11 ± 0.01	1.68 ± 0.19	1.05 ± 0.04
20%	2.07 ± 0.29	40.76 ± 0.85	12.25 ± 1.34	0.62 ± 0.05	0.39 ± 0.05	5.02 ± 0.22	1.96 ± 0.04

Our data also showed that there was a reduced production of ethanol and an increased production of metabolites including lactate and acetoin under aerobic conditions (Figure 2, Table 2). *Z. mobilis* growth reached its peak after 24-h cultivation under aerobic conditions with a dramatic production increment of acetoin. Acetoin titers rose above 5 g/L when fermentation was performed in 100-mL shake flask with 20 mL medium. Glucose was completely consumed under anaerobic conditions at the end of fermentation. However, glucose was not completely consumed with high titers of byproducts such as acetoin, glycerol and lactate under aerobic conditions, which could be due to the low NADH/NAD+ ratio and therefore the inefficient glycolysis and cellular growth under aerobic conditions.

3.2. Identification and Construction of Heterogeneous Acetoin Biosynthetic in Z. mobilis

als, *aldC*, and *butA* genes related to the acetoin biosynthesis pathway were selected for investigation. An online NCBI tblastn was performed against the *Z. mobilis* chromosomal and native plasmid sequences [29]. Our result indicated that the gene encoding AldC is absent in *Z. mobilis* and ZMO0687, ZMO1139, ZMO1140 of *Z. mobilis* have high similarity to the catabolic enzyme Als. Further analysis indicates that ZMO1139/ZMO1140 (*ilvB/C*) may form a complex involved in the branched-chain amino acids pathway. In addition, the Als homologue ZMO0687 may compete for the substrate (pyruvate) binding and utilization with ZMO1139/ZMO1140 complex and pyruvate decarboxylase (PDC, ZMO1360) for acetolactate accumulation.

BLAST results show that *Z. mobilis* possesses three ButA homologs ZMO0318, ZMO1_ZMOp33x016, ZMO1_ZMOp39x008, of which, ZMO1_ZMOp33x016, and ZMO1_ZMOp39 x008 are from native plasmids. Those enzymes may contribute to the conversion of diacetyl to acetoin. *Z. mobilis* has three *als* gene homologs, while the absence of *aldC* gene hinders the synthase of acetoin; therefore, the heterologous *aldC* gene is indispensable in our pathway engineering strategy. To improve acetoin production, an optimized gene *aldC* from *E. cloacae* and an *als* gene from *B. licheniformis* with high affinity were introduced to compete with PDC and shift the carbon flux from ethanol production (Figure 3). Moreover, *noxE* gene encoding the NADH oxidase was used to redirect the NADH flux from respiration to improved growth under aerobic conditions.

The gene expression cassettes containing the sequences of acetoin pathway genes (*als*, *aldC*, *noxE*) were synthesized. And several plasmid constructs were generated for investigation (Figure 3A). Those constructs were then transferred to *Z. mobilis* by electroporation. The engineered strains with corresponding plasmids were cultured in 100-mL shake flasks with 20 mL medium at 100 rpm. When fermented with glucose, *Z. mobilis* can produce abundant acetoin together with ethanol and byproducts of lactate, acetate, and glycerol in the NADH-dependent metabolic pathways under aerobic conditions (Figure 3C).

Results indicated that the introduction of an individual optimized *aldC* enhanced the acetoin production, and the titer of acetoin increased by 15% (Figure 3C). A high affinity *als* gene was assembled, and it was helpful to improve acetoin titer. The titer of acetoin increased by 24% to 6.23 g/L compared to the original strain. The introduction of the heterologous *noxE* gene remarkably increased acetoin production to 6.87g/L with the decrease in lactate (Figure 3). Moreover, the product of ethanol was also enhanced in the engineered strains. The introduction of the acetoin biosynthetic pathway into ZM4;

therefore, it may reduce the lactate formation through the efficient conversion of pyruvate to acetoin and then relieve the growth defects. In addition, the consumption rate of glucose in ZM4 (pEZ-AldC-Als-NoxE) was 4.18 $g \cdot L^{-1} \cdot h^{-1}$, which was more efficient than the control strain ZM4 (pEZ) (Figure 3, Table 3). This result suggested that more glucose was allocated to produce end products rather than to be consumed by respiration.

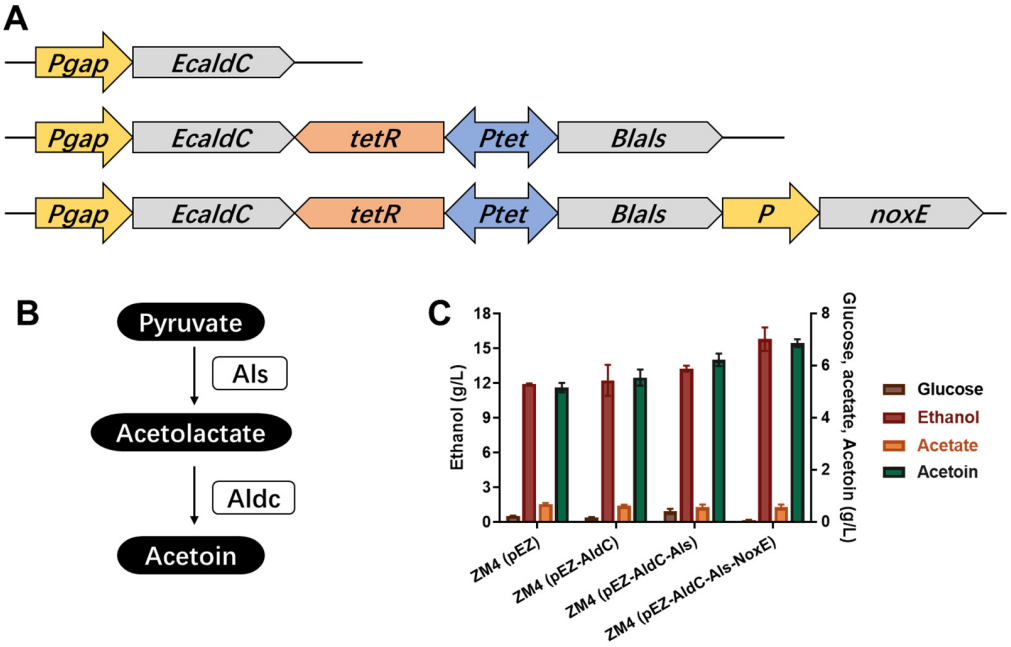


Figure 3. Strategy and result of metabolic engineering of *Z. mobilis* ZM4 for acetoin production. (**A**) Three plasmids designed for the acetoin pathway genes were tested in *Z. mobilis*. *Pgap*, a native promoter of *Z. mobilis*; *EcaldC*, *aldC* from *E. cloacae*, *Blals*, *als* gene from *B. licheniformis*. (**B**) Schematic of heterogenous acetoin biosynthetic pathway. (**C**) Metabolites produced by different recombinant strains of *Z. mobilis* containing different combinations of heterologous genes. Values are the means of experiments with three or more technical replicates; error bars are standard deviations.

Table 3. Fermentation profiles of recombinant *Z. mobilis* strains containing different gene(s) for acetoin biosynthesis. GCR: Glucose consumption rate, GC: Glucose consumed. Strains were cultured in 100-mL shake flakes with 20 mL medium at 30 °C, 100 rpm. Mean values for triplicate repeats are shown for each condition ± standard deviation.

Strains	GCR ($g \cdot L^{-1} \cdot h^{-1}$)	GC ($g \cdot L^{-1}$)	Ethanol ($g \cdot L^{-1}$)	Acetate ($g \cdot L^{-1}$)	Glycerol ($g \cdot L^{-1}$)	Acetoin ($g \cdot L^{-1}$)	Lactate ($g \cdot L^{-1}$)
ZM4 (pEZ)	2.24 ± 0.11	38.90 ± 0.20	11.95 ± 0.03	0.69 ± 0.04	0.13 ± 0.01	5.16 ± 0.18	1.33 ± 0.04
ZM4 (pEZ-AldC)	2.17 ± 0.33	38.99 ± 0.62	12.25 ± 1.34	0.52 ± 0.03	0.15 ± 0.01	5.55 ± 0.31	0.92 ± 0.08
ZM4 (pEZ-AldC-Als)	2.41 ± 0.10	41.45 ± 0.39	13.25 ± 0.25	0.57 ± 0.13	0.19 ± 0.05	6.23 ± 0.24	0.36 ± 0.05
ZM4 (pEZ-AldC-Als-NoxE)	4.18 ± 0.21	47.20 ± 0.54	15.8 ± 1.02	0.57 ± 0.11	0.23 ± 0.02	6.87 ± 0.15	0.05 ± 0.01

3.3. Recovery of Redox Imbalance by Expressing NADH Oxidase

To resolve the redox imbalance, a water-forming NADH oxidase under the control of *pdc* promoter was integrated into the acetoin biosynthetic plasmid pEZ15Asp resulting in pEZ-NoxE. The recombinant strain ZM4 (pEZ-NoxE) showed a significant improvement in glucose consumption rate under aerobic conditions and took less time to completely ferment 50 g/L glucose than that of wild-type ZM4. Moreover, acetoin production was improved up to 5.97 g/L under the 20% bottle volume suggesting that the redox imbalance caused by acetoin production was alleviated by expressing NADH oxidase NoxE (Table 4).

Table 4. Fermentation profiles of the recombinant strain ZM4 (pEZ-NoxE) containing NADH oxidase NoxE under different conditions. GCR: Glucose consumption rate, GC: Glucose consumed. Strains were cultured in 100-mL shake flakes with 20 mL medium at 30 °C, 100 rpm. Mean values for triplicate repeats are shown for each condition ± standard deviation.

Volume	GCR ($g \cdot L^{-1} \cdot h^{-1}$)	GC ($g \cdot L^{-1}$)	Ethanol ($g \cdot L^{-1}$)	Acetate ($g \cdot L^{-1}$)	Glycerol ($g \cdot L^{-1}$)	Acetoin ($g \cdot L^{-1}$)	Lactate ($g \cdot L^{-1}$)
80%	4.15 ± 0.08	46.38 ± 0.04	20.12 ± 0.07	0.14 ± 0.01	0.29 ± 0.02	2.16 ± 0.15	0.82 ± 0.05
50%	4.16 ± 0.14	45.52 ± 0.16	19.16 ± 0.15	0.13 ± 0.00	0.36 ± 0.01	2.76 ± 0.11	0.66 ± 0.05
20%	4. 11 ± 0.20	41.96 ± 0.75	14.34 ± 0.46	0.28 ± 0.03	0.45 ± 0.02	5.97 ± 0.03	0.00 ± 0.00

Oxygen supply can significantly affect the ratio of NADH/NAD^+. To confirm the effect of NoxE expression on redox state, we analyzed intracellular NAD^+/NADH ratios in wild-type ZM4 and recombinant strain ZM4 (pEZ-NoxE). As expected, the NAD^+/NADH ratios in recombinants were higher than those in the wild type under different fermentation conditions, demonstrating the efficient conversion of NADH to NAD^+ by NoxE (Figure 4). In *Z. mobilis*, NAD^+ regeneration for glycolysis is mainly achieved by producing ethanol. By introducing an acetoin synthesis pathway, NADH will be accumulated. And the introduction of NoxE can help regenerate NAD^+ from NADH leading to cofactor rebalance.

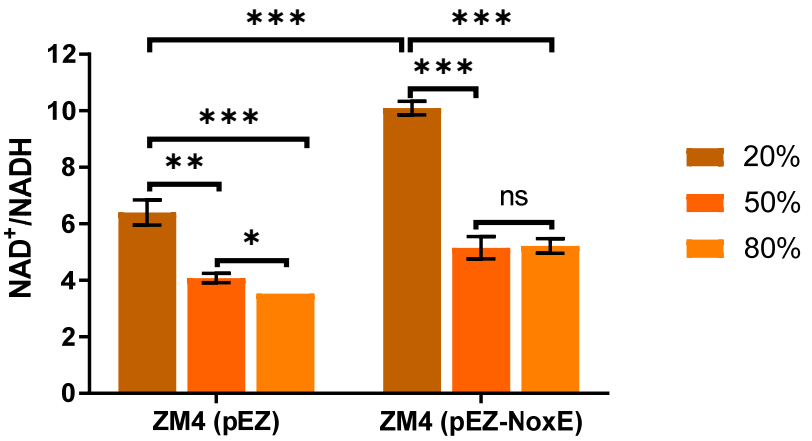


Figure 4. The NAD^+/NADH ratios in the recombinant strains of ZM4 (pEZ) and ZM4 (pEZ-NoxE) strains. Strains were cultured in 100-mL shake flakes containing 20 mL (20%), 50 mL (50%) and 80 mL (80%) medium at 30 °C, 100 rpm. Values are the means of experiments with three or more technical replicates, and error bars are standard deviations. A *p*-value less than 0.05 is considered to be statistically significant (* $p < 0.05$; ** $p < 0.01$; *** $p < 0.001$). ns: not significant.

3.4. Optimization of Fermentation Conditions for Acetoin Production

To achieve high concentrations of acetoin, different oxygen supplies were also investigated by varying the shaking speeds. Growth conditions with different shaking speeds and medium volumes affected oxygen dispersion; therefore, they impacted acetoin production (Figure 5). The titer of acetoin rose above 8.84 g/L when the shaking speed was increased to 200 rpm with 20 mL medium in the 100-mL shake flask. with a yield of 0.36 g/g glucose, reaching 35% of the maximum theoretical yield. Accordingly, recombinant strain ZM4 (pEZ-AldC-Als-NoxE) exhibited about a two-fold increase in acetoin productivity (0.34 $g \cdot L^{-1} \cdot h^{-1}$) compared with wild type (0.19 $g \cdot L^{-1} \cdot h^{-1}$), suggesting that redox imbalance caused by acetoin production was successfully alleviated by expressing NADH oxidase.

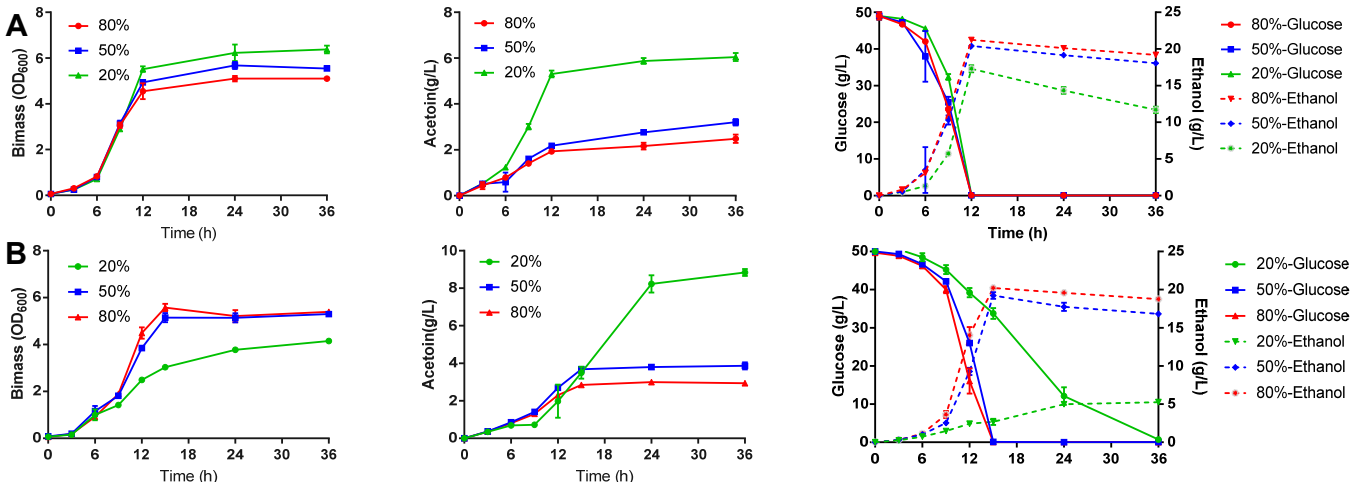


Figure 5. Growth curve and fermentation profiles of the recombinant strain ZM4 (pEZ-AldC-Als-NoxE) cultured in flasks with the shaking speed of 100 rpm (**A**) or 200 rpm (**B**). Values are the means of experiments with three or more technical replicates, and error bars are standard deviations.

3.5. Increase in Acetoin Production by Redirecting Carbon Source from Ethanol Production

Redirection of the carbon flux to acetoin production by regulating redox balance: The respiratory chain of *Z. mobilis* consists of type-II NAD(P)H dehydrogenase (ZMO1113, Ndh), ubiquinone-10 (Q_{10}), and a cytochrome bd-type ubiquinol oxidase (ZMO1571, ZMO1572) [30,31]. An NADH dehydrogenase deficiency mutant was constructed to investigate the effect of Ndh on NADH and carbon flux redirection. The *ndh* in ZM4 (pEZ-AldC-Als-NoxE) was knocked out using type I−F CRISPR−Cas system. Our results showed that the biomass of *ndh* deficient strain under aerobic conditions was significantly improved (Figure 6A). The titer of acetoin increased by 50% while the titer of ethanol decreased by 20%, indicated that the carbon flux of *ndh* deficient mutant was redirected to acetoin production from ethanol (Figure 6B), which is consistent with previous reports that the knockout of *ndh* stimulated the redirection of the NADH flux from respiration to the production of catabolic products including acetoin and improved cell growth under aerobic conditions in *Z. mobilis* [30,31].

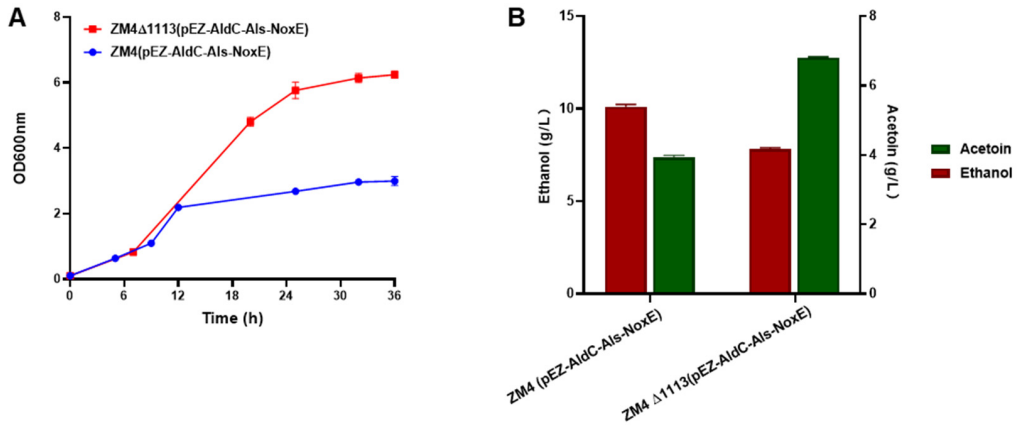


Figure 6. Growth curve (**A**) as well as the titers of ethanol and acetoin (**B**) of the recombinant strain ZM4 (pEZ-AldC-Als-NoxE) and ZM4 Δ1113(pEZ-AldC-Als-NoxE) cultured in flasks with the shaking speed of 200 rpm. Values are the means of experiments with three or more technical replicates, error bars are standard deviation.

Redistribution of the carbon flux to acetoin production from ethanol by CRISPRi: The inducible promoter Ptet has been identified to be a compatible biological part for

Z. mobilis [21]. In this work, the TetR system was employed to construct the inducible CRISPR/dCas12 system for gene interference in *Z. mobilis*. The TetR-dCas12a was intergraded into the genome of ZM (pEZ-AldC-Als-NoxE) by replacing the native gene ZMO1759 (Table 1).

A sgRNA was then designed targeting *pdc* gene encoding pyruvate decarboxylase. The tunable CRISPRi was used to redirect carbon flux from ethanol to acetoin production by inhibiting the *pdc* expression using the CRISPRi system. Our results demonstrated that the interference of *pdc* through CRISPRi improved the acetoin production although its growth was affected (Figure 7A), and the titer of acetoin increased by 11.24% while the titer of ethanol decreased by 15.57% (Figure 7B,C). The correlation of acetoin production with ethanol production, and the correlation of tetracycline with acetoin production and ethanol production were then investigated. Our results indicated that the reduction of ethanol was positively correlated with the production of acetoin (Figure 7D), and the production of acetoin and ethanol had a linear correlation with the gradient of tetracycline concentrations (Figure 7E,F), as the production of acetoin was enhanced correspondingly to the increase in the tetracycline inducer concentrations, whereas the production of ethanol was decreased correspondingly to the increase in the tetracycline inducer concentrations within 0–1.2 μg/mL.

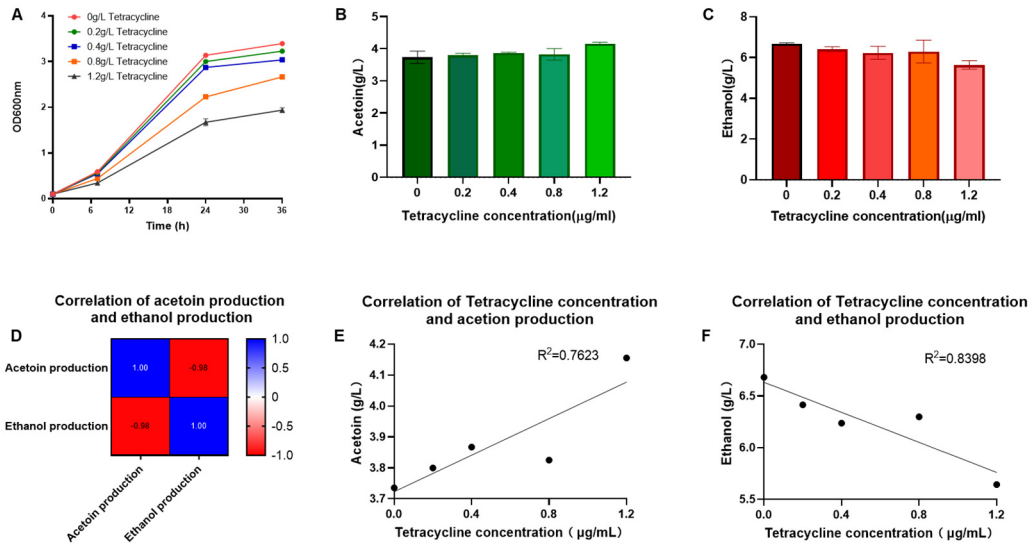


Figure 7. Growth curve (**A**), acetoin (**B**) and ethanol (**C**) production of the recombinant strain ZM4−1759dCas12a (pEZ-AldC-Als-NoxE), as well as the correlation of acetoin production with ethanol production (**D**), the correlation of tetracycline with acetoin (**E**) and ethanol (**F**) production. dCas12a−based CRISPRi system of *Z. mobilis* was applied to redirect the carbon flux from ethanol production to acetoin biosynthesis, which includes dCas12a controlled by the inducible promoter P*tetR* that was stably integrated into the ZMO1759 locus, and the editing plasmid containing a constitutively expressed sgRNA targeting *pdc*. Cells were cultured in flasks with the shaking speed of 200 rpm supplemented with different concentrations of the inducer tetracycline. Values are the means of experiments with three or more technical replicates, error bars are standard deviation.

Considering the effectiveness of both strategies on redirecting carbon flux into acetoin production from ethanol biosynthesis, a combinational approach will be carried out to further redirect of the carbon flux to acetoin production in the future.

4. Discussion

Z. mobilis is a highly efficient ethanol-producing bacterium with a small genome size and desirable industrial characteristics, which makes it a promising chassis for biorefinery and synthetic biology studies [18,32,33]. The genome sequence and functional

re-annotation as well as substantial genome editing toolboxes of *Z. mobilis* were well documented [29,34,35]. Additionally, the recombinant *Z. mobilis* strains broaden the capability of fermentable substrates to both hexose and pentose sugars, which is regarded as having great promise for bioproducts from lignocellulosic biomass [36–38]. All of these works help better understand the application and development of *Z. mobilis* as a suitable chassis for biochemical production.

As a promising ethanologenic organism for large-scale bio-ethanol production, *Z. mobilis* is the only known microorganism so far to utilize the Entner-Doudoroff (ED) pathway anaerobically for sugar fermentation, which endows it with an improved ethanol yield [9,20]. *Z. mobilis* possesses a truncated tricarboxylic acid (TCA) cycle due to the lack of two key TCA cycle enzymes. In the absence of oxygen, most NADH is used for ethanol production, and ethanol is the primary product. However, acetoin is more abundant during aerobic fermentation with low biomass under aerobic conditions, and there is competition between the respiratory chain and alcohol dehydrogenase for NADH oxidation. O_2 inhibits alcohol dehydrogenase, which leads to inefficient conversion of acetaldehyde to ethanol and the disturbance of the cellular NADH/NAD^+ ratios. NADH dehydrogenase transfers electrons from NADH to ubiquinone ($Q_{10}H_2$) and the flux of cofactor to ethanol product was then reduced [24,25]. *Z. mobilis* possesses an active respiratory chain containing the components of the type II NADH dehydrogenase (Ndh), coenzyme Q10, and the cytochrome bd terminal oxidase. Inhibition of respiration with cyanide, or inactivation of the respiratory NADH dehydrogenase (Ndh) can prevent the accumulation of the inhibitory metabolite acetaldehyde resulting in enhanced aerobic growth [24,25].

Currently, acetoin is mostly produced via aerobic conversion of sugar compounds. However, acetoin is an oxidized product, which necessitates the addition of an external electron acceptor if acetoin is supposed to be the only product formed in this process. Moreover, the enhanced acetoin-producing pathway will exacerbate the cofactor imbalance. The water-forming NADH oxidase (NoxE) is an intermediary to transfer electrons to the acceptor oxygen under aerobic conditions. In this study, a significant improvement in glucose consumption rate and acetoin production for the recombinant strain ZM4 (pEZ-AldC-Als-NoxE) under aerobic conditions suggested that the redox imbalance caused by acetoin production was successfully alleviated by expressing NADH oxidase.

In addition, the carbon flux distributions between cell growth and respiration under aerobic conditions or recombinant strains with cofactor imbalance could cause lower product yield than the theoretical ones. The alleviation of this by expressing the NADH oxidase NoxE also suggested that the deletion of *ndh* to avoid NADH oxidization and the overexpression of NoxE to accelerate NADH to NAD^+ conversion could help increase NAD^+ accumulation; therefore, the efficient glycolysis for normal cell growth. Since inducible promoters and many promoters with different strengths were identified, and genome−editing toolkits including the native type I−F CRISPR−Cas system and the CRISPR−Cas12 system have been established in *Z. mobilis* [26,27], the synthetic genetic cluster containing genes for target biochemical biosynthesis and genes for cofactor balance such as *noxE* for NADH/NAD^+ conversion and *zwf* for NADH/NADPH conversion can be further designed rationally and then integrated into the genome of *Z. mobilis* for the construction of efficient microbial cell factories.

5. Conclusions

Harnessing the power of microorganisms to produce value-added chemicals from renewable resources offers a promising alternative to current industrial processes. In this study, acetoin production in *Z. mobilis* was improved by introducing genes for heterologous acetoin biosynthesis and cofactor balance. Our results revealed that oxygen supplies affected the NADH/NAD^+ ratio, and the cofactor imbalance generated during acetoin production was successfully alleviated by expressing NADH oxidase, leading to significantly enhanced acetoin production. This work thus demonstrated that modulating NADH/NAD^+ ratio could be an effective engineering strategy, and the exploration of

enzymes related to redox reactions and respiratory chain will facilitate the construction of efficient microbial cell factories for the cost-effective biochemical production in the future.

Author Contributions: Conceptualization: S.Y. and J.D., methodology: W.S., S.Y. and W.B., investigation and validation: W.S., W.B. and Q.P., formal analysis and data curation: W.S., W.B. and S.Y., writing: W.S., W.B., J.D. and S.Y., supervision and project administration: S.Y. All authors have read and agreed to the published version of the manuscript.

Funding: Supported by the National Natural Science Foundation of China (U1932141 and 21978071), 2022 Joint Projects between Chinese and CEEC's Universities (202004), the National Key Technology Research and Development Program of China (2022YFA0911800 and 2018YFA0900300), the Leading Innovative and Entrepreneur Team Introduction Program of Zhejiang Province (2018R01014), and the Innovation Base for Introducing Talents of Discipline of Hubei Province (2019BJH021). Funding was also supported by the State Key Laboratory of Biocatalysis and Enzyme Engineering.

Institutional Review Board Statement: Not applicable.

Informed Consent Statement: Not applicable.

Data Availability Statement: All data were included.

Acknowledgments: We acknowledge the support from the State Key Laboratory of Biocatalysis and Enzyme Engineering.

Conflicts of Interest: The authors declare no conflict of interest.

References

1. Xiao, Z.; Xu, P. Acetoin metabolism in bacteria. *Crit. Rev. Microbiol.* **2007**, *33*, 127–140. [CrossRef] [PubMed]
2. Bursac, T.; Gralnick, J.A.; Gescher, J. Acetoin production via unbalanced fermentation in *Shewanella oneidensis*. *Biotechnol. Bioeng.* **2017**, *114*, 1283–1289. [CrossRef] [PubMed]
3. Xiao, Z.; Lu, J.R. Strategies for enhancing fermentative production of acetoin: A review. *Biotechnol. Adv.* **2014**, *32*, 492–503. [CrossRef]
4. Li, S.; Gao, X.; Xu, N.; Liu, L.; Chen, J. Enhancement of acetoin production in *Candida glabrata* by in silico-aided metabolic engineering. *Microb. Cell Factories* **2014**, *13*, 55. [CrossRef] [PubMed]
5. Renna, M.C.; Najimudin, N.; Winik, L.R.; Zahler, S.A. Regulation of the *Bacillus subtilis alsS, alsD,* and *alsR* genes involved in post-exponential-phase production of acetoin. *J. Bacteriol.* **1993**, *175*, 3863–3875. [CrossRef]
6. Zhang, Y.; Li, S.; Liu, L.; Wu, J. Acetoin production enhanced by manipulating carbon flux in a newly isolated *Bacillus amyloliquefaciens*. *Biores. Technol.* **2013**, *130*, 256–260. [CrossRef]
7. Zhang, L.; Liu, Q.; Ge, Y.; Li, L.; Ma, C. Biotechnological production of acetoin, a bio-based platform chemical, from lignocellulosic resource by metabolically engineered *Enterobacter cloacae*. *Green Chem.* **2016**, *18*, 1560–1570. [CrossRef]
8. Sun, J.A.; Zhang, L.Y.; Rao, B.; Shen, Y.L.; Wei, D.Z. Enhanced acetoin production by *Serratia marcescens* H32 with expression of a water-forming NADH oxidase. *Bioresour. Technol.* **2012**, *119*, 94–98. [CrossRef]
9. He, M.X.; Wu, B.; Qin, H.; Ruan, Z.Y.; Tan, F.R.; Wang, J.L.; Shui, Z.X.; Dai, L.C.; Zhu, Q.L.; Pan, K.; et al. *Zymomonas mobilis*: A novel platform for future biorefineries. *Biotechnol. Biofuels* **2014**, *7*, 101. [CrossRef]
10. Bae, S.J.; Kim, S.; Hahn, J.S. Efficient production of acetoin in *Saccharomyces cerevisiae* by disruption of 2,3-butanediol dehydrogenase and expression of NADH oxidase. *Sci. Rep.* **2016**, *6*, 27667. [CrossRef]
11. Liu, L.; Xu, Q.M.; Chen, T.; Cheng, J.S.; Yuan, Y.J. Artificial consortium that produces riboflavin regulates distribution of acetoin and 2,3-butanediol by *Paenibacillus polymyxa* CJX518. *Eng. Life Sci.* **2017**, *17*, 1039–1049. [CrossRef] [PubMed]
12. Magee, R.J.; Kosaric, N. The microbial production of 2,3-butanediol. *Adv. Appl. Microbiol.* **1987**, *32*, 89–161.
13. Hugenholtz, J.; Kleerebezem, M.; Starrenburg, M.; Delcour, J.; de Vos, W.; Hols, P. *Lactococcus lactis* as a cell factory for high-level diacetyl production. *Appl. Environ. Microbiol.* **2000**, *66*, 4112–4114. [CrossRef] [PubMed]
14. Wu, Y.G.; Chang, A.K.; Nixon, P.F.; Li, W.; Duggleby, R.G. Mutagenesis at *asp27* of pyruvate decarboxylase from *Zymomonas mobilis*: Effect on its ability to form acetoin and acetolactate. *Eur. J. Biochem.* **2000**, *267*, 6493–6500. [CrossRef]
15. Chen, G.C.; Jordan, F. Brewers' yeast pyruvate decarboxylase produces acetoin from acetaldehyde: A novel tool to study the mechanism of steps subsequent to carbon dioxide loss. *Biochemistry* **1984**, *23*, 3576–3582. [CrossRef]
16. Jörnvall, H.; Persson, B.; Krook, M.; Atrian, S.; Gonzalez-Duarte, R.; Jeffery, J.; Ghosh, D. Short-chain dehydrogenases/reductases (SDR). *Biochemistry* **1995**, *34*, 6003–6013. [CrossRef]
17. Kallberg, Y.; Oppermann, U.; Jörnvall, H.; Persson, B. Short-chain dehydrogenases/reductases (SDRs) Coenzyme-based functional assignments in completed genomes. *Eur. J. Biochem.* **2002**, *269*, 4409–4417. [CrossRef]
18. Qiu, M.; Shen, W.; Yan, X.; He, Q.; Cai, D.; Chen, S.; Wei, H.; Knoshaug, E.P.; Zhang, M.; Himmel, M.E.; et al. Metabolic engineering of *Zymomonas mobilis* for anaerobic isobutanol production. *Biotechnol. Biofuels* **2020**, *13*, 15. [CrossRef]

19. Wang, X.; He, Q.; Yang, Y.; Wang, J.; Haning, K.; Hu, Y.; Wu, B.; He, M.; Zhang, Y.; Bao, J.; et al. Advances and prospects in metabolic engineering of *Zymomonas mobilis*. *Metab. Eng.* **2018**, *50*, 57–73. [CrossRef]
20. Yang, S.; Fei, Q.; Zhang, Y.; Contreras, L.M.; Utturkar, S.M.; Brown, S.D.; Himmel, M.E.; Zhang, M. *Zymomonas mobilis* as a model system for production of biofuels and biochemicals. *Microb. Biotechnol.* **2016**, *9*, 699–717. [CrossRef]
21. Yang, S.; Mohagheghi, A.; Franden, M.A.; Chou, Y.C.; Chen, X.; Dowe, N.; Himmel, M.E.; Zhang, M. Metabolic engineering of *Zymomonas mobilis* for 2,3-butanediol production from lignocellulosic biomass sugars. *Biotechnol. Biofuels* **2016**, *9*, 189. [CrossRef] [PubMed]
22. Rao, B.; Zhang, L.Y.; Sun, J.; Su, G.; Wei, D.; Chu, J.; Zhu, J.; Shen, Y. Characterization and regulation of the 2,3-butanediol pathway in *Serratia marcescens*. *Appl. Microbiol. Biotechnol.* **2012**, *93*, 2147–2159. [CrossRef]
23. Mayer, D.; Schlensog, V.; Böck, A. Identification of the transcriptional activator controlling the butanediol fermentation pathway in *Klebsiella terrigena*. *J. Bacteriol.* **1995**, *177*, 5261–5269. [CrossRef]
24. Hayashi, T.; Furuta, Y.; Furukawa, K. Respiration-deficient mutants of *Zymomonas mobilis* show improved growth and ethanol fermentation under aerobic and high temperature conditions. *J. Biosci. Bioeng.* **2011**, *111*, 414–419. [CrossRef] [PubMed]
25. Kalnenieks, U.; Galinina, N.; Strazdina, I.; Kravale, Z.; Pickford, J.L.; Rutkis, R.; Poole, R.K. NADH dehydrogenase deficiency results in low respiration rate and improved aerobic growth of *Zymomonas mobilis*. *Microbiology* **2008**, *154*, 989–994. [CrossRef]
26. Shen, W.; Zhang, J.; Geng, B.; Qiu, M.; Hu, M.; Yang, Q.; Bao, W.; Xiao, Y.; Zheng, Y.; Peng, W.; et al. Establishment and application of a CRISPR-Cas12a assisted genome-editing system in *Zymomonas mobilis*. *Microb. Cell Factories* **2019**, *18*, 162. [CrossRef]
27. Zheng, Y.; Han, J.; Wang, B.; Hu, X.; Li, R.; Shen, W.; Ma, X.; Ma, L.; Yi, L.; Yang, S.; et al. Characterization and repurposing of the endogenous Type I-F CRISPR-Cas system of *Zymomonas mobilis* for genome engineering. *Nucleic Acids Res.* **2019**, *47*, 11461–11475. [CrossRef]
28. Yang, S.; Tschaplinski, T.J.; Engle, N.L.; Carroll, S.L.; Martin, S.L.; Davison, B.H.; Palumbo, A.V.; Rodriguez, M., Jr.; Brown, S.D. Transcriptomic and metabolomic profiling of *Zymomonas mobilis* during aerobic and anaerobic fermentations. *BMC Genom.* **2009**, *10*, 34. [CrossRef] [PubMed]
29. Yang, S.; Vera, J.M.; Grass, J.; Savvakis, G.; Moskvin, O.V.; Yang, Y.; McIlwain, S.J.; Lyu, Y.; Zinonos, I.; Hebert, A.S.; et al. Complete genome sequence and the expression pattern of plasmids of the model ethanologen *Zymomonas mobilis* ZM4 and its xylose-utilizing derivatives 8b and 2032. *Biotechnol. Biofuels* **2018**, *11*, 125. [CrossRef]
30. Lou, J.; Wang, J.; Yang, Y.; Yang, Q.; Li, R.; Hu, M.; He, Q.; Du, J.; Wang, X.; Li, M.; et al. Development and characterization of efficient xylose utilization strains of *Zymomonas mobilis*. *Biotechnol. Biofuels* **2021**, *14*, 231. [CrossRef]
31. Hayashi, T.; Kato, T.; Furukawa, K. Respiratory chain analysis of *Zymomonas mobilis* mutants producing high levels of ethanol. *Appl. Environ. Microbiol.* **2012**, *78*, 5622–5629. [CrossRef]
32. Hu, M.; Chen, X.; Huang, J.; Du, J.; Li, M.; Yang, S. Revitalizing the ethanologenic bacterium *Zymomonas mobilis* for sugar reduction in high-sugar-content fruits and commercial products. *Bioresour. Bioprocess.* **2021**, *8*, 119. [CrossRef] [PubMed]
33. Li, Y.; Wang, Y.; Wang, R.; Yan, X.; Wang, J.; Wang, X.; Chen, S.; Bai, F.; He, Q.; Yang, S. Metabolic engineering of *Zymomonas mobilis* for continuous co-production of bioethanol and poly-3-hydroxybutyrate (PHB). *Green Chem.* **2022**, *24*, 2588–2601. [CrossRef]
34. Yang, S.; Pan, C.; Hurst, G.B.; Dice, L.; Davison, B.H.; Brown, S.D. Elucidation of *Zymomonas mobilis* physiology and stress responses by quantitative proteomics and transcriptomics. *Front. Microbiol.* **2014**, *5*, 246. [CrossRef]
35. Yang, S.; Pan, C.; Tschaplinski, T.J.; Hurst, G.B.; Engle, N.L.; Zhou, W.; Dam, P.; Xu, Y.; Rodriguez, M., Jr.; Dice, L.; et al. Systems biology analysis of *Zymomonas mobilis* ZM4 ethanol stress responses. *PLoS ONE* **2013**, *8*, e68886. [CrossRef]
36. Zhang, M.; Eddy, C.; Deanda, K.; Finkelstein, M.; Picataggio, S. Metabolic engineering of a pentose metabolism pathway in ethanologenic *Zymomonas mobilis*. *Science* **1995**, *267*, 240–243. [CrossRef]
37. Yang, Y.; Hu, M.; Tang, Y.; Geng, B.; Qiu, M.; He, Q.; Chen, S.; Wang, X.; Yang, S. Progress and perspective on lignocellulosic hydrolysate inhibitor tolerance improvement in *Zymomonas mobilis*. *Bioresour. Bioprocess.* **2018**, *5*, 6. [CrossRef]
38. Strazdina, I.; Kravale, Z.; Galinina, N.; Rutkis, R.; Poole, R.K.; Kalnenieks, U. Electron transport and oxidative stress in *Zymomonas mobilis* respiratory mutants. *Arch. Microbiol.* **2012**, *194*, 461–471. [CrossRef]

Disclaimer/Publisher's Note: The statements, opinions and data contained in all publications are solely those of the individual author(s) and contributor(s) and not of MDPI and/or the editor(s). MDPI and/or the editor(s) disclaim responsibility for any injury to people or property resulting from any ideas, methods, instructions or products referred to in the content.